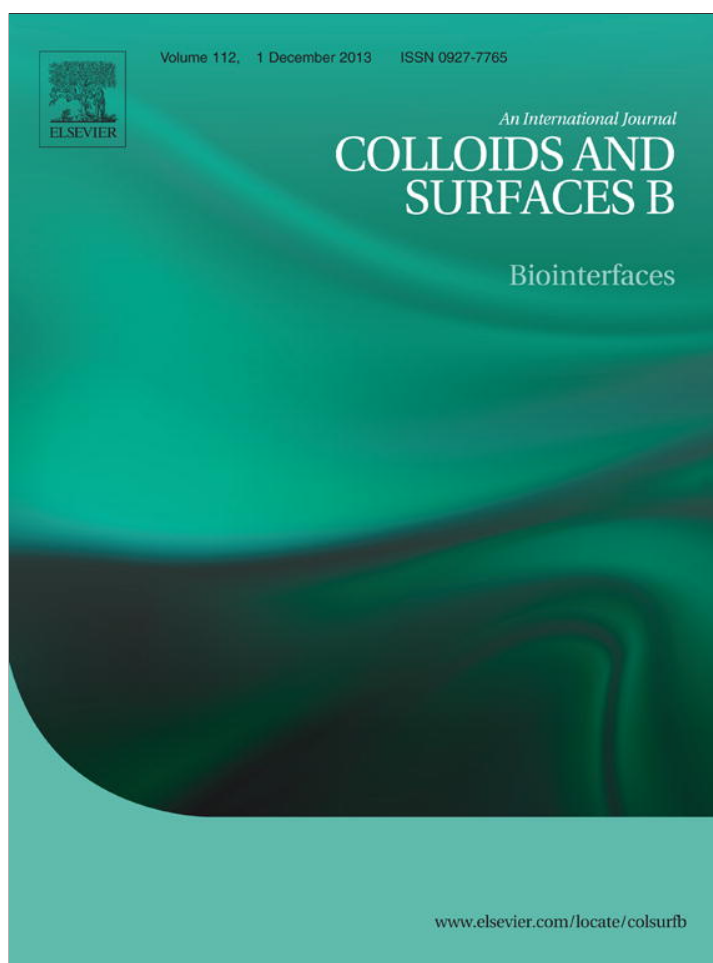


Provided for non-commercial research and education use.  
Not for reproduction, distribution or commercial use.



This article appeared in a journal published by Elsevier. The attached copy is furnished to the author for internal non-commercial research and education use, including for instruction at the authors institution and sharing with colleagues.

Other uses, including reproduction and distribution, or selling or licensing copies, or posting to personal, institutional or third party websites are prohibited.

In most cases authors are permitted to post their version of the article (e.g. in Word or Tex form) to their personal website or institutional repository. Authors requiring further information regarding Elsevier's archiving and manuscript policies are encouraged to visit:

<http://www.elsevier.com/authorsrights>



Contents lists available at ScienceDirect

## Colloids and Surfaces B: Biointerfaces

journal homepage: [www.elsevier.com/locate/colsurfb](http://www.elsevier.com/locate/colsurfb)

## Preparation and characterization of DNA/allophane composite hydrogels



Takuya Kawachi, Yoko Matsuura, Fumitoshi Iyoda, Shuichi Arakawa, Masami Okamoto\*

Advanced Polymeric Nanostructured Materials Engineering, Graduate School of Engineering Toyota Technological Institute, 2-12-1 Hisakata, Tempaku, Nagoya 468 8511, Japan

## ARTICLE INFO

## Article history:

Received 2 May 2013

Received in revised form 5 July 2013

Accepted 8 August 2013

Available online 23 August 2013

## Keywords:

Natural allophane

Double-stranded DNA

Adsorption

Hydrogels

Thermal denaturation

## ABSTRACT

The preparation and characterization of the composite hydrogels based on double-stranded deoxyribonucleic acid (DNA) and natural allophane (AK70) were reported. To understand the propensity of the natural allophane to adsorb the DNA molecules, using zeta potential measurement, Fourier transform infrared spectroscopy (FTIR) and electrophoresis analyses assessed the adsorption characteristics. The freeze-dried DNA/AK70 hydrogels were demonstrated that the DNA bundle structure with a width of  $\sim 2 \mu\text{m}$  and a length of  $\sim 15\text{--}20 \mu\text{m}$  was wrapped around the clustered allophane particles as revealed by FE-SEM/EDX analysis. The incorporation of AK70 in hydrogels induced the increase in the enthalpy of the helix-coil transition of DNA duplex due to the restricted molecular motions of the DNA duplex facilitated by the interaction between the phosphate groups of DNA and the protonated  $^+(\text{OH}_2)\text{Al}(\text{OH}_2)$  groups on the wall perforations of the allophane.

© 2013 Elsevier B.V. All rights reserved.

## 1. Introduction

Hydrogels are hydrophilic, three-dimensional networks, which are able to imbibe large amounts of water or biological fluids, and thus resemble, to a large extent, a biological tissue. They are insoluble due to the presence of chemical (tie-points, junctions) and/or physical crosslinks such as entanglements, crystallites and phase separation. These materials can be synthesized to respond to a number of physiological stimuli present in the body, such as pH, ionic strength and temperature [1,2]. Some clay was used in the formulation of hydrogels [3] and pH-sensitive properties [4,5].

In another design, deoxyribonucleic acid (DNA) sequences have been frequently used as biorecognition motifs in the design of new biohydrogels [6–8]. In this direction, we have investigated the adsorption characteristics of single-stranded DNA (ss-DNA) on clay particles [9].

Allophane is a short-range-order clay mineral and occurs in some soils derived from volcanic ejecta. The primary particle of the allophane is a hollow spherule with an outer diameter of 3.5–5.0 nm and a wall about 0.6–1.0 nm thick, which has perforations as shown in Fig. 1 [10,11]. Allophane was used as an adsorbent. The surface area of allophane is as high as  $\sim 1000 \text{ m}^2 \text{ g}^{-1}$ , which is often larger than activated carbon. In addition to this large surface area, the  $(\text{OH})\text{Al}(\text{OH}_2)$  groups exposed on the

wall perforations are the source of the pH-dependent charge characteristics of allophane [10,11].

After adsorption of DNA molecules on the allophane surface, the hydrogel was formed in the clustered allophane particles. However, the detail of the structure development and the process of gelation are not fully revealed yet [9]. The objective of this study is the analysis of propensity of the natural allophane to adsorb the DNA molecules. We discussed the structure development of DNA/allophane hydrogels.

Knowledge of such hydrogels based on DNA molecules and natural allophane clusters should also be useful in the conception of new forms of drugs release with highly-specific dosage and an improvement of the technological and biopharmaceutical properties in polymer/clay nanocomposite hydrogels [12–21].

## 2. Experimental

## 2.1. Materials

The allophane sample was provided by Shinagawa Chemicals Ltd. and designated as AK70. AK70 was not further purified for use. The overall size of a single allophane particle is  $\sim 5 \text{ nm}$  with a surface area of  $250 \text{ m}^2 \text{ g}^{-1}$  [9], which was estimated by the *t*-method [22].

The double-stranded DNA, sodium salt from salmon testes was purchased from Sigma–Aldrich (D1626). The Guanine–Cytosine (G–C) content was reported to be 41.2%. The melting temperature was  $87.5 \text{ }^\circ\text{C}$  in 0.15 M sodium chloride and 0.015 M sodium citrate. The molecular weight was 1300 kDa possessing ca. 2000 base pair (bp).

\* Corresponding author. Tel.: +81 528091861; fax: +81 528091864.

E-mail address: [okamoto@toyota-ti.ac.jp](mailto:okamoto@toyota-ti.ac.jp) (M. Okamoto).

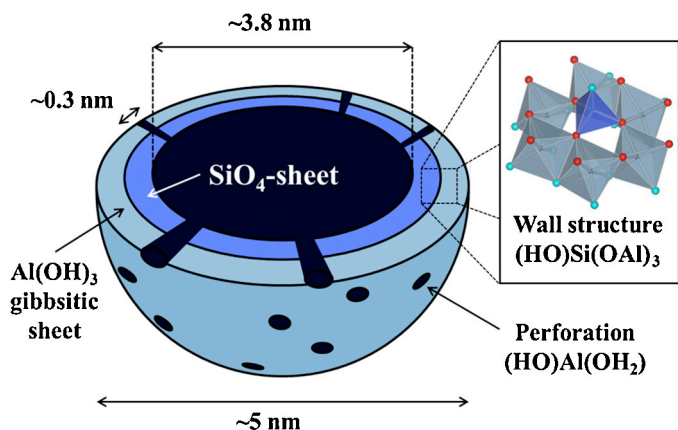


**Fig. 1.** Schematic representation of allophane structure. The overall size of a single allophane particle is  $\sim 5$  nm. The pore-size distribution of AK70 shows a peak at  $\sim 1.9$  nm [11].

## 2.2. Adsorption experiments

The DNA was mixed in different AK70 wt. ratio (DNA/AK70 = 10/90–90/10, corresponding to DNA concentration = 0.011–0.90 wt%) with Millipore Milli-Q ultrapure (18 M $\Omega$  cm, total organic carbon (TOC) < 20 ppb) water. In addition, 5–10  $\mu$ L of dilute HCl (Nacalai Tesque) solution was added in each solutions and adjusted to the pH 4.0. Millipore Milli Q water through dialysis membrane was used without Tris–HCl buffer solution for all experiments [23]. The solutions were shaken well for 72 h at room temperature. 72 h was fixed as the equilibrium time throughout this study because adsorption uptake approached the constant value, as revealed by our previous paper [9]. After equilibrating DNA adsorption (hydrogel formation) [9], the supernatant solutions were collected after centrifuge at a speed of 5000 rpm for 20 min. The total organic carbon (TOC) and total nitrogen (TN) of supernatant solutions were measured by using combustion method with a set temperature of 800  $^{\circ}$ C after four point calibration using an analytik jana multiN/C 2100S instrument [9].

The sediments (hydrogels designated as DNA/AK70) were also collected to analyze the interaction between phosphate groups of DNA molecules and functional Al–OH groups on the allophane particles.

For morphological observation and thermal analysis, freeze-drying (FDU-2200, Eyela Ltd.) of DNA/AK70 hydrogels was performed under 10 Pa at  $-80$   $^{\circ}$ C for 10 h.

## 2.3. Characterization

The morphological features of the freeze-dried DNA/AK70 hydrogels were observed through field emission scanning electron microscopy (FE-SEM) (SU6600, Hitachi Ltd.) equipped with elemental analysis by energy dispersive X-ray spectrometry (EDX) (INCA x-act, Oxford Instruments). The operated accelerating voltage was 5 kV without any metal coating of the sample surface. The contrast of FE-SEM images depend on the atomic number of each object, therefore, Si and Al atoms are much more highlighted than organic DNA molecules in these experiments.

The freeze-dried DNA/AK70 hydrogels were also characterized by using temperature-modulated differential scanning calorimetry (TMDSC) (TA 2920; TA Instruments) at the heating rate of 5  $^{\circ}$ K/min with a heating rate of the modulation period ( $\Delta$ ) of 60 s and an amplitude ( $T_{amp}$ ) of  $\pm 0.769$  K from  $-50$  to 180  $^{\circ}$ C, to determine the melting temperature ( $T_m$ ) and calorimetric enthalpy ( $\Delta H$ ). The

TMDSC was calibrated with Indium before experiments [24]. We have estimated the value of the excess heat capacity ( $C_p$ ) of helix-coil transition during thermal denaturation as a heat absorption peak of the duplex melting [25]. By considering the heat flow amplitude ( $Q_{amp}$ ), the heat capacity was evaluated by the following equation.

$$C_p = -K_{cp} \left( \frac{Q_{amp}}{T_{amp}} \right) \left( \frac{\Delta}{2\pi} \right) \quad (1)$$

where  $K_{cp}$  is the thermal capacity constant (=1.023). All measurements were performed for four replicates and averaged to get the final value.

Fourier transform infrared (FTIR) spectra were collected at 1  $cm^{-1}$  nominal resolution using a FTIR spectrometer (FT-730, Horiba Ltd.) equipped with ZnSe mull omni-cell window (GS01834, Specac Co., UK) in transmission mode. The spectra were obtained by averaging 25 scans with a mean collection length of 1 s per spectrum. The background spectra used for reduction were collected with sample. By subtracting the spectrum of AK70 from the consecutive spectra of DNA/AK70 hydrogels, a difference spectrum was processed by software.

The surface charge characteristics of AK70 or DNA molecules in water (0.1 wt%) were determined by electrophoresis (Zetasizer Nano ZS, Malvern Instruments, UK) by the technique of laser Doppler anemometry. The method involved washing AK70 several times with water and adjusting the pH of the suspension in the range of 1–12 using dilute HNO<sub>3</sub> (Nacalai Tesque) and NaOH (Nacalai Tesque). All measurements were performed for four replicates and averaged to get the final value.

Electrophoresis was performed using microchip electrophoresis system (MultiNA, Shimadzu Co.) in 10 mM Tris–HCl buffer solution without polymerase chain reaction. The samples prepared from the supernatant solutions were 0.5–1.0 ng/ $\mu$ L with the addition of 50 mM KCl and 1.5 mM MgCl<sub>2</sub>. The DNA ladder indicators for a standard range from 100 to 10,002 bps were used to judge the electropherograms.

## 3. Results and discussion

### 3.1. Surface charge characteristics and adsorption properties

Based on the morphology of the allophane, AK70 sample, Fig. 1 shows the probable structure of the spherule wall, the wall perforations, and the intra-spherule void. The overall size of a single allophane particle is  $\sim 5$  nm. The surface charge characteristics of allophane is very different from that of DNA. Allophane has a variable or pH-dependent surface charge, because the (HO)Al(OH<sub>2</sub>) groups, exposed at surface defect sites, can either acquire or lose protons depending on the pH of the ambient solution. They become <sup>+</sup>(OH<sub>2</sub>)Al(OH<sub>2</sub>) by acquiring protons on the acid side of the point of zero charge (PZC), and become (OH)Al(OH)<sup>-</sup> by losing protons on the alkaline side [26]. The results of the zeta potential measurements of AK70 are shown in Fig. 2. The PZC of AK70 was (pH)  $\sim 6$ . In the pH range of 2–11, both positively and negatively charged species are present on the surface of allophane particle [26].

The phosphate groups of DNA molecules possess a negative charge (PO<sub>2</sub><sup>-</sup>). The zeta potential values for the surface of the DNA are negative over the entire pH range from 3 to 11 and even more smaller negative ( $\sim -40$  mV) at a lower pH value, which may be attributed by the acquiring protons to the phosphate groups on the acid side. Furthermore, the values decrease with increasing continuously to attain  $-100$  mV at pH 9.72. Beyond pH 10.0, the zeta potential values increase again, presumably due to the differently charged two substituted purine groups [27].

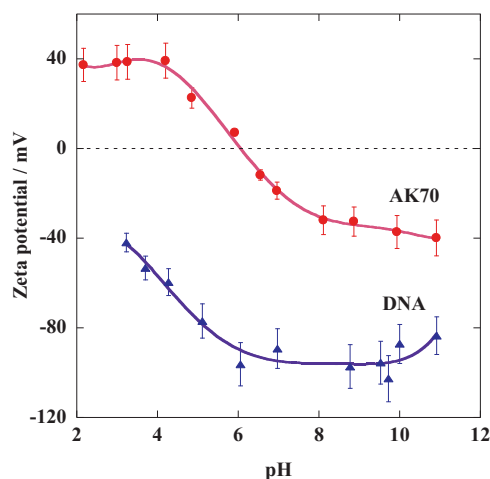


**Fig. 2.** Zeta potential versus pH of AK70 and DNA. Point of zero charge of AK70 is (pH) ~6.0. Results are expressed as mean  $\pm$  S.D. ( $n=4$ ).

The adsorption features of DNA on AK70 at pH 4.0 were examined to clarify the interaction generated between the phosphate groups and the Al-OH groups (Fig. 3). At lower feed concentration of AK70 (0.004–0.05 wt% in water), the adsorption capacity of DNA by AK70 exhibits a much larger value (~90% adsorption) than that at higher concentration of AK70 in feed (0.1–2.1 wt% in water). The higher feed AK70 concentration significantly reduces the adsorption (~20% adsorption) due to the clustered allophane particles, which are formed in water [9]. The DNA molecules can more easily adsorb on the large surface area of AK70 particles at lower feed concentration of AK70. Consequently, DNA feed content in lower AK70 concentration leads to the high DNA content in hydrogel. As a matter of course, the interstitial spaces of the clustered particles may play an important role of the adsorption of DNA molecules. In our previous paper [9], the adsorption isotherms of DNA by AK70 were characterized by the Freundlich equation. The relative adsorption capacity and adsorption intensity were discussed in terms of the temperature dependence of the adsorption.

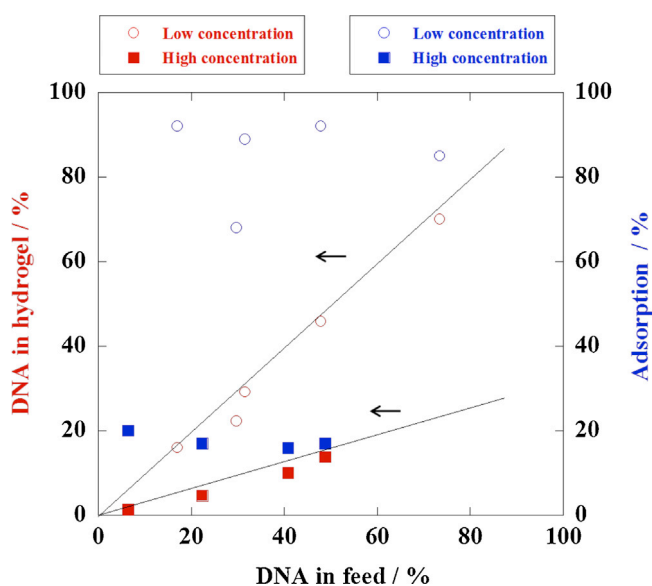


**Fig. 3.** DNA content in hydrogels and DNA adsorption % for lower (red) and higher feed AK70 concentrations (blue) as a function of DNA in feed after adsorption by AK70 at room temperature at pH 4.0. (For interpretation of the references to color in figure legend, the reader is referred to the web version of the article.)

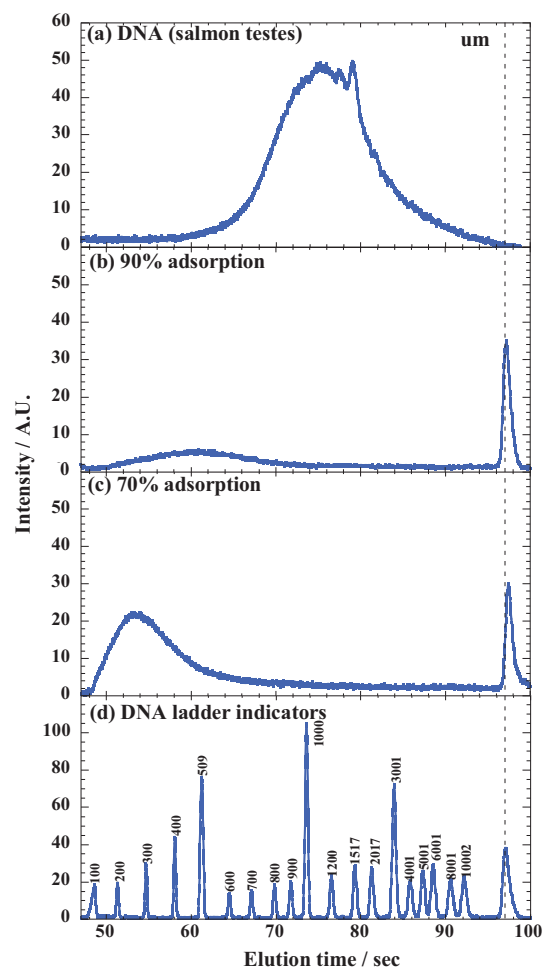


**Fig. 4.** Electropherogram of (a) pristine DNA (salmon testes), supernatant solution of (b) 90% adsorption of DNA and (c) 70% adsorption of DNA, and (d) DNA ladder indicators range from 100 to 10,002 bps. The dashed line represents the upper marker ( $\mu\text{m}$ ). The lower marker (lm) appears precisely at the elution time of 44.5 s (data not shown).

Using electrophoresis analysis we observed that the structure of DNA is changed upon adsorption on the AK70 surfaces. Before adsorption of the pristine DNA, the appearance of main peak is observed at 1500bp having size range from 700 to 10,000bps, whereas the remnant shoulder is located around 100–700 bps size (Fig. 4a). As conjectured, the distribution is broad owing to the heterogeneous base composition of the salmon testes DNA. For the supernatant solution of 90% adsorption of DNA, the elution profile in the electropherogram remains the short bps around the DNA ladder indicators for a standard range from 100 to 900 bps (Fig. 4b). The electropherogram for 70% adsorption exhibits the profile similar to that of 90% adsorption (Fig. 4c). The peak mainly consists of short molecule for a standard range from 200 to 400 bps where it appears. The reason is not obvious at present. However, what is striking in our observation is the magnitude of the mobility of DNA molecules on the surfaces of AK70 for the desorption process. Thus, we need to consider the possibility that the short bps in DNA cause desorption of the DNA molecules from the allophane surfaces.

### 3.2. Electrostatic interaction in hydrogels

The functional groups Al-OH exposed on the wall perforations of allophane is protonated with a lower pH value (=4.0) of the medium. The phosphate groups of DNA possess a negative charge ( $\text{PO}_2^-$ ), which bind directly to the protonated  $^+(\text{OH}_2)\text{Al}(\text{OH}_2)$  groups

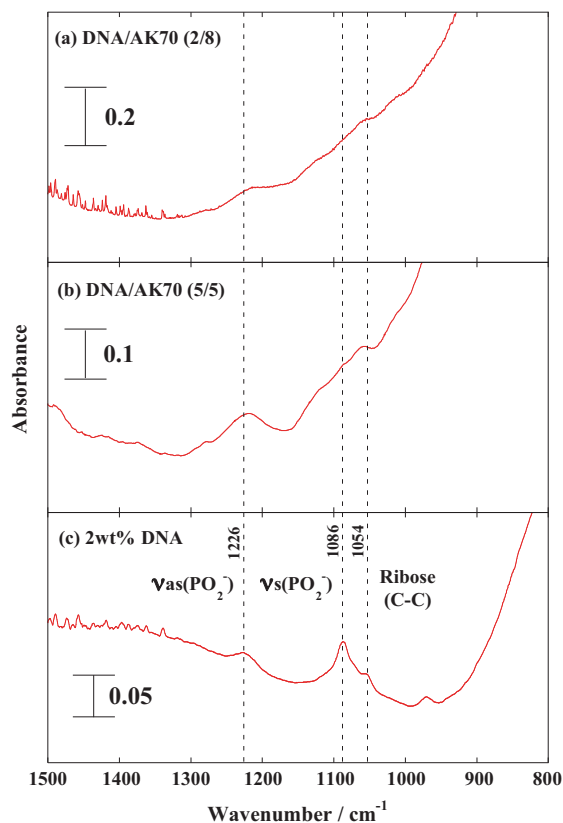


**Fig. 5.** FTIR difference spectra of (a) DNA/AK70 (2/8) and (b) DNA/AK70 (5/5) hydrogels recovered from the sediment, and (c) 2 wt% DNA aqueous solution in the region of 800–1500  $\text{cm}^{-1}$ .

through an electrostatic interaction leading to an increased adsorption. Thus, the adsorption ability of allophanes is highly depended on the interactions of phosphate and (OH)Al(OH)<sub>2</sub> groups through protonation with a varying pH.

The frequencies and the vibrational assignments for the DNA with B-form are reported in the literature [28]. The sensitive bands at 1226  $\text{cm}^{-1}$  (asymmetric stretching mode of  $\text{PO}_2^-$  groups:  $\nu_{\text{as}}(\text{PO}_2^-)$ ), 1086  $\text{cm}^{-1}$  (symmetric stretching mode:  $\nu_{\text{s}}(\text{PO}_2^-)$ ) and 1054  $\text{cm}^{-1}$  (stretching of ribose  $\nu(\text{C}-\text{C})$ ) of the phosphodiester-deoxyribose backbone provide valuable information to understand the interaction generated between DNA backbone and allophane surfaces. By subtracting the spectrum of AK70 from the consecutive spectra of DNA/AK70 hydrogels recovered from the sediment with ca. 20 and ca. 50 wt% DNA at pH 4, a difference spectrum was obtained (Fig. 5). The presence of the sensitive bands in the difference spectrum is also confirmed. We notice that  $\nu_{\text{as}}(\text{PO}_2^-)$  band shifts to the lower frequency side from 1226 to 1220  $\text{cm}^{-1}$ . In contrast, the variation of  $\nu_{\text{s}}(\text{PO}_2^-)$  exhibits nearly constant. The formation of the interaction between  $\text{PO}_2^-$  groups of DAN and AK70 surfaces was suggested.

### 3.3. Morphological feature of freeze-dried hydrogels

The FE-SEM images of freeze-dried hydrogels clearly reveal the clustered or agglomerated particles range of 10–20  $\mu\text{m}$ , which are rather than singular particles (a diameter of  $\sim 5$  nm, Fig. 6). We see that the clustered allophane particles are connected each other to form the network structure in water. The FE-SEM image of DNA/AK70 (2/8) hydrogel at the same area shows that the C (green), N (purple) and P (light blue) atoms derived from DNA molecules and Al (red), Si (blue) and Fe (brown) corresponding to AK70 are distributed on the agglomerated particles as revealed by EDX mapping

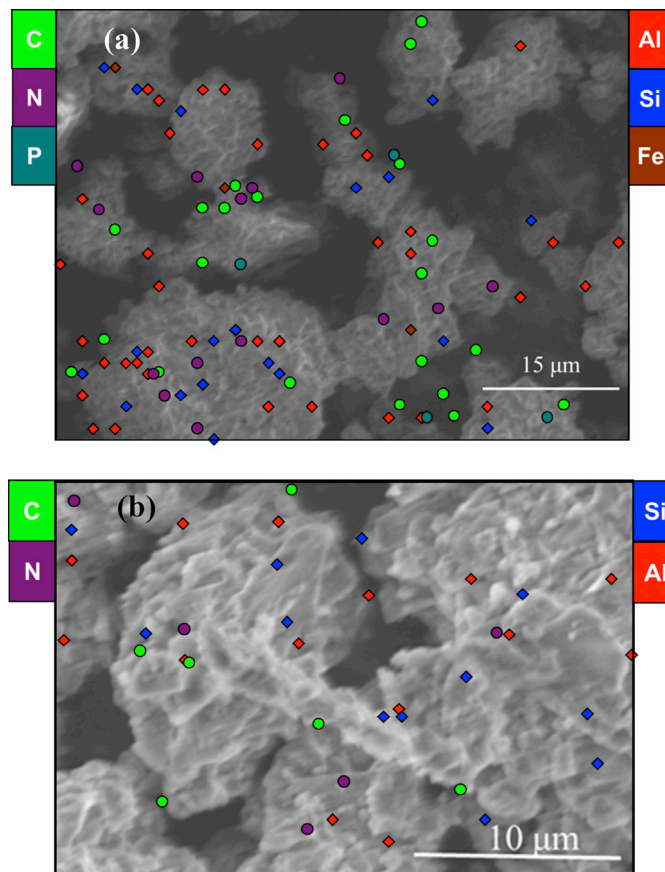


**Fig. 6.** FE-SEM images showing freeze-dried (a) DNA/AK70 (2/8) and (b) DNA/AK70 (5/5) hydrogels. EDX mapping at the same areas for C (green), N (purple) and P (light blue) atoms derived from DNA, and Al (red), Si (blue) and Fe (brown) corresponding to AK70. (For interpretation of the references to color in figure legend, the reader is referred to the web version of the article.)

(Fig. 6a). The EDX spectrum of AK70 confirms the presence of impurities such as Fe-containing minerals. The DNA molecules are probably more readily covered by the agglomerated particles of allophane because the negative charges of DNA molecules are neutralized by the immobilized positive charges of the allophane surfaces.

For the image of DNA/AK70 (5/5) hydrogel (Fig. 6b), we see that the DNA bundle structure with a width of  $\sim 2$   $\mu\text{m}$  and a length of  $\sim 15$ –20  $\mu\text{m}$  rather than single DNA tubes (a diameter and length of 2 and 680 nm, respectively [23]) is generated beside the clustered allophane particles. The C, N and Si atoms are also distributed on the structure, suggesting that the DNA molecules are wrapped around the allophane clusters. The DNA bundle structure may play an important role of the intertwined network formation in hydrogels.

### 3.4. Thermal denaturation of DNA molecules in freeze-dried hydrogels

The effect of temperature upon the DNA duplex was investigated by DSC, which measures the heat absorbed during thermal denaturation and melting transition [29]. By monitoring the progress of the transition, the TMDSC measurement provides the  $T_m$  and associated changes in the calorimetric heat capacity.

Fig. 7 shows the temperature-induced unfolding (helix-coil transition) of the DNA duplex in the hydrogels after freeze-drying. As expected, the melting transition of freeze-dried DNA (red) is broad owing to the heterogeneous base composition of the salmon testes DNA, as mentioned above. The excess heat capacity curve of

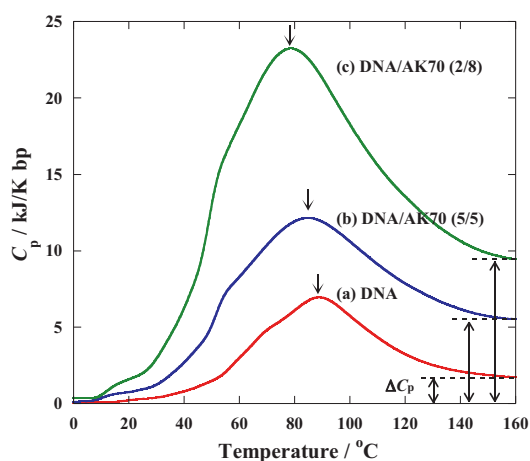


**Fig. 7.** TMDSC thermograms for freeze-dried (a) pristine DNA, (b) DNA/AK70 (5/5) and (c) DNA/AK70 (2/8) hydrogels. Arrows on the excess heat capacity curves indicate melting temperatures.  $\Delta C_p$  is obtained as a baseline-derived gap.

**Table 1**

Thermodynamic parameters of freeze-dried DNA/AK70 hydrogels and pristine DNA (salmon testes). Results are expressed as mean  $\pm$  S.D. ( $n=4$ ).

Samples	$\Delta H$ (kJ bp <sup>-1</sup> ) <sup>a</sup>	$T_m$ (°C)
DNA/AK70 (2/8)	1024 $\pm$ 25	77.8 $\pm$ 0.4
DNA/AK70 (5/5)	585 $\pm$ 18	83.8 $\pm$ 0.3
DNA	321 $\pm$ 16	88.5 $\pm$ 0.5
DNA (in aq. solution) <sup>b</sup>	28	75.5

<sup>a</sup> The values are calculated per base pair (bp).

<sup>b</sup> The value is measured in an aqueous solution (containing 5 mM sodium cacodylate) of DNA having 160  $\pm$  5 bp (5%, w/w) at pH 6.5 and reported by Duguid et al. [25].

three examined DNA duplexes melting develops from rather high temperature and is somewhat asymmetric as compared to that of the helix-coil transition of DNA duplex (160  $\pm$  5 bp) in an aqueous solution of 5 mM sodium cacodylate at pH 6.5 [25]. The values of  $T_m$  and calorimetric enthalpy ( $\Delta H$ ) per bp of three examined DNA duplexes, i.e., pristine and DNA/AK70 hydrogels are summarized in Table 1. In case of the freeze-dried DNA duplex, the calculated value of  $\Delta H$  is one order of magnitude greater than that of DNA duplex in an aqueous solution [25], probably due to the transition in solid-state. Obviously, the thermal denaturation is strongly affected by the restricted solid-state. The suppression of the melting (increase of  $\Delta H$ ) may be ascribed to the restricted molecular motions of the DNA duplex in bulk. This feature is much enhanced in DNA/AK70 hydrogels. The value of  $\Delta H$  reflects the importance of the interaction generated between phosphate groups of DNA molecules and functional Al-OH groups on the allophane wall perforations. For the DNA duplexes in DNA/AK70 hydrogels, the strand dissociation occurs in the further region of the endotherm, judging by its sharpness (blue for DNA/AK70 (5/5) and green for DNA/AK70 (2/8), respectively). The  $T_m$  values as a heat absorption peak slightly decreases with increasing AK70 content in hydrogel. Other interesting feature is the non-zero (positive) heat capacity change ( $\Delta C_p$ ) accompanying the helix-coil transition observed in the DSC thermograms. The  $\Delta C_p$  for the melting is significant to discuss the changes in enthalpy and entropy for the helix-coil transition [30]. Such discussion is beyond the objective of this paper, and we will report it separately [31].

#### 4. Conclusions

In this study, we have demonstrated the structure development of hydrogels composed of DNA molecules and clustered allophane

particles in aqueous solution. The adsorption of DNA at pH 4 was facilitated by the interaction between the phosphate groups of DNA and the protonated  $^+(\text{OH}_2)\text{Al}(\text{OH}_2)$  groups on the wall perforations of the allophane as revealed by FTIR analysis. Owing to the clustered allophane particles, lower feed concentration of AK70 led to the high DNA content in hydrogel. The adsorption morphologies consisting of the bundled DNA and the clustered allophane particles were successfully observed through FE-SEM/EDX analysis. The DNA bundle structure with a width of  $\sim 2 \mu\text{m}$  and a length of  $\sim 15\text{--}20 \mu\text{m}$  is generated beside the clustered allophane particles after preparation of the freeze-dried hydrogels. The DNA molecules are wrapped around the allophane clusters. In addition, the incorporation of AK70 in hydrogels induced the increase in the enthalpy of the helix-coil transition of DNA duplex, which was ascribed to the restricted molecular motions of the DNA duplex due to the strong affinity between DNA and AK70.

#### Acknowledgments

This work was supported by the Grant in TTI as a Special Research Project (2012–2013) and the Strategic Research Infrastructure Project of the Ministry of Education, Sports, Science and Technology, Japan (2010–2014).

#### References

- [1] N.A. Peppas, P. Bures, W. Leobandung, H. Ichikawa, Hydrogels in pharmaceutical formulations, *Eur. J. Pharm. Biopharm.* 50 (2000) 27–46.
- [2] C.C. Lin, A.T. Metters, Hydrogels in controlled release formulations: network design and mathematical modeling, *Adv. Drug Deliv. Rev.* 58 (2006) 1379–1408.
- [3] W.F. Lee, Y.C. Chen, Effect of bentonite on the physical properties and drug-release behavior of poly(AA-co-PEGMEA)/bentonite nanocomposite hydrogels for mucoadhesive, *J. Appl. Polym. Sci.* 91 (2004) 2934–2941.
- [4] X. Huang, S. Xu, M. Zhong, J. Wang, S. Feng, R. Shi, Modification of Na-bentonite by polycations for fabrication of amphoteric semi-IPN nanocomposite hydrogels, *Appl. Clay Sci.* 42 (2009) 455–459.
- [5] Q. Wang, J. Zhang, A. Wang, Preparation and characterization of a novel pH-sensitive chitosan-g-poly(acrylic acid)/attapulgate/sodium alginate composite hydrogel bead for controlled release of diclofenac sodium, *Carbohydr. Polym.* 78 (2009) 731–737.
- [6] Y. Murakami, M. Maeda, DNA-responsive hydrogels that can shrink or swell, *Biomacromolecules* 6 (2005) 2927–2929.
- [7] C.A. Mirkin, R.L. Letsinger, R.C. Mucic, J.J. Storhoff, A DNA-based method for rationally assembling nanoparticles into macroscopic materials, *Nature* 382 (1996) 607–609.
- [8] V.T. Milam, A.L. Hiddessen, J.C. Crocker, D.J. Graves, D.A. Hammer, DNA-driven assembly of biodisperse, micron-sized colloids, *Langmuir* 19 (2003) 10317–10323.
- [9] Y. Matsuura, F. Iyoda, S. Arakawa, B. John, M. Okamoto, H. Hayashi, DNA adsorption characteristics of hollow spherule allophane nano-particles, *Mater. Sci. Eng. C* (2013) (in press).
- [10] M.F. Brigatti, E. Galan, B.K.G. Theng, Structures and mineralogy of clay mineral, in: F. Bergaya, B.K.G. Theng, G. Lagaly (Eds.), *Handbook of Clay Science*, Elsevier, Amsterdam, 2006, pp. 19–86.
- [11] F. Iyoda, S. Hayashi, S. Arakawa, M. Okamoto, Synthesis and adsorption characteristics of hollow spherical allophane nano-particles, *Appl. Clay Sci.* 56 (2012) 77–83.
- [12] K. Campbell, D.Q.M. Craig, T. McNally, Poly(ethylene glycol) layered silicate nanocomposites for retarded drug release prepared by hot-melt extrusion, *Int. J. Pharm.* 363 (2008) 126–131.
- [13] X. Wang, Y. Du, J. Luo, Biopolymer/montmorillonite nanocomposite: preparation, drug-controlled release property and cytotoxicity, *Nanotechnology* 19 (2008) 1–7.
- [14] G.R. Silva, E. Ayres, R.L. Orefice, S.A. Moura, D.C. Cara, S. Cunha Ada Jr., Controlled release of dexamethasone acetate from biodegradable and biocompatible polyurethane and polyurethane nanocomposite, *J. Drug Target.* 17 (2009) 374–383.
- [15] C. Ribeiro, G.G.C. Arizaga, F. Wypych, M.R. Sierakowski, Nanocomposites coated with xyloglucan for drug delivery: in vitro studies, *Int. J. Pharm.* 367 (2009) 204–210.
- [16] T.R. Thatiparti, S. Tammishetti, M.V. Nivasu, UV curable polyester polyol acrylate/bentonite nanocomposites: synthesis, characterization, and drug release, *J. Biomed. Mater. Res. B* 92 (2010) 111–119.
- [17] Q. Yuan, J. Shah, S. Hein, R.D.K. Misra, Controlled and extended drug release behavior of chitosan-based nanoparticle carrier, *Acta Biomater.* 6 (2010) 1140–1148.
- [18] B.D. Kevadiya, G.V. Joshi, H.C. Bajaj, Layered bionanocomposites as carrier for procainamide, *Int. J. Pharm.* 388 (2010) 280–286.

- [19] L. Perioli, V. Ambrogi, L. di Nauta, M. Nocchetti, C. Rossi, Effects of hydrotalcite-like nanostructured compounds on biopharmaceutical properties and release of BCS class II drugs: the case of flurbiprofen, *Appl. Clay Sci.* 51 (2011) 407–413.
- [20] I. Salcedo, C. Aguzzi, G. Sandri, M.C. Bonferoni, M. Mori, P. Cerezo, R. Sanchez, C. Viseras, C. Caramella, In vitro biocompatibility and mucoadhesion of montmorillonite chitosan nanocomposite: a new drug delivery, *Appl. Clay Sci.* 55 (2012) 131–137.
- [21] B.D. Kevadiya, T.A. Patel, D.D. Jhala, R.P. Thumbar, H. Brambhatt, M.P. Pandya, S. Rajkumar, P.K. Jena, G.V. Joshi, P.K. Gadhia, C.B. Tripathi, H.C. Bajaj, Layered inorganic nanocomposites: a promising carrier for 5-fluorouracil(5-FU), *Eur. J. Pharm. Biopharm.* 81 (2012) 91–101.
- [22] B.C. Lippens, J.H. de Boer, Studies on pore systems in catalysts: V. The t method, *J. Catalysis* 4 (1965) 319–323.
- [23] A. Taki, B. John, S. Arakawa, M. Okamoto, Structure and rheology of nanocomposite hydrogels composed of DNA and clay, *Eur. Polym. J.* 49 (2012) 923–931.
- [24] S. Sinha Ray, K. Yamada, M. Okamoto, Y. Fujimoto, A. Ogami, K. Ueda, New polylactide/layered silicate nanocomposites. 5. Designing of materials with desired properties, *Polymer* 44 (2003) 6633–6646.
- [25] J.G. Duguid, V.A. Bloomfield, J.M. Benevides, G.J. Thomas Jr., DNA melting investigated by differential scanning calorimetry and Raman spectroscopy, *Biophys. J.* 71 (1996) 3350–3360.
- [26] G. Yuan, S.I. Wada, Allophane and imogolite nanoparticles in soil and their environmental applications, in: A.S. Barnard, H.B. Guo (Eds.), *Nature's Nanostructures*, Pan Stanford Publishing Pte. Ltd., Singapore, 2012, pp. 485–508.
- [27] J.A. Schellman, D. Stigter, Electrical double layer, zeta potential, and electrophoretic charge of double-stranded DNA, *Biopolymers* 16 (1977) 1415–1434.
- [28] S.H. Brewer, S.J. Anthireya, S.E. Lappi, D.L. Drapcho, S. Franzen, Detection of DNA hybridization on gold surfaces by polarization modulation infrared reflection absorption spectroscopy, *Langmuir* 18 (2002) 4460–4464.
- [29] K.J. Breslauer, E. Freire, M. Straume, Calorimetry: a tool for DNA and ligand-DNA studies, *Methods Enzymol.* 211 (1992) 533–567.
- [30] A. Tikhomirova, N. Taulier, T.V. Chalikian, Energetics of nucleic acid stability: the effect of  $\Delta C_p$ , *J. Am. Chem. Soc.* 126 (2004) 16387–16394.
- [31] Y. Matsuura, S. Arakawa, M. Okamoto. 2013 (in preparation).